



Taguchi's methodology of optimizing turning parameters over chip thickness ratio in machining P/M AMMC

T. Tamizharasan¹ · N. Senthilkumar² · V. Selvakumar³ · S. Dinesh⁴

© Springer Nature Switzerland AG 2019

Abstract

Effect of turning parameters on chip generation during machining aluminum composite is studied in this work. Turning of Al–4%Cu–7.5%SiC composite material prepared through powder metallurgy procedure was chosen as the workpiece, machined using uncoated carbide insert TNMG 120404. Chips produced during machining were studied by measuring the thickness and were used along with uncut chip thickness to determine the chip thickness ratio. 99.85% pure aluminum was added with 4% volume fractions of copper and with silicon carbide particulates of 7.5%. To visualize the distribution of reinforcement phases in matrix, scanning electron microscope is used. Taguchi's methodology of design of experiments was adopted for designing a L_9 (Latin square) orthogonal array for experimental investigation, and from analysis of variance, cutting speed influencing the formation of chip by 64.13%, continuing with depth of cut by 35.26%, was identified. Confirmation test accomplished with ideal conditions produces a better chip condition.

Keywords Aluminum MMC · Taguchi's technique · Powder metallurgy · ANOVA · Confidence interval

1 Introduction

Metal matrix composites (MMCs) were specifically used where the situation needs high strength combined with toughness and ductility and can be used at elevated operating temperatures up to 1260 °C. The ductile material that can be selected as matrix may be one among the materials such as copper, aluminum, titanium, magnesium, superalloy, nickel, or even intermetallic compounds, and the reinforcements can be ceramic particulars such as alumina, boron carbide and silicon carbide and fibers like graphite. Compared with engineering materials, composite materials provide higher strength and stiffness exclusively at higher temperature, enhanced fatigue resistance, wear and abrasion and lower coefficient of thermal expansion. When compared with organic matrix materials, composite materials offer improved thermal and electrical conductivity and higher resistance to heat. Figure 1 shows a

comparison, certainly for explanatory purposes, among the composite materials and conventional monolithic materials, viz., steel and aluminum [1].

Maximum amount of commercial works toward MMCs has concentrated on aluminum as the matrix material. It is selected mainly due to the properties such as environmental resistance, light weight, and useful mechanical characteristics have made aluminum alloys very popular; and these qualities also mark aluminum appropriate for usage as matrix material [2]. The melting temperature of aluminum is sufficiently high for satisfying numerous application necessities; however, it is little adequate to render the procedure of preparing composite, practically suitable. Similarly, aluminum can accommodate a diversity of reinforcing agents. Discontinuous reinforcements that mainly consist of Al_2O_3 , SiC, B_4C , TiN and TiC were added to matrix, and MMCs are produced primarily by stir (vortex/mixing) casting and powder metallurgy (PM) processing

✉ N. Senthilkumar, nsk@adhiparasakthi.in | ¹Green Pearl India (Pvt.) Ltd, Kattangulathur, Tamil Nadu 603203, India. ²Adhiparasakthi Engineering College, Melmaruvathur, Tamil Nadu 603319, India. ³Srinivasan Engineering College, Perambalur, Tamil Nadu 621212, India. ⁴K. Ramakrishnan College of Technology, Tiruchirappalli, Tamil Nadu 621112, India.



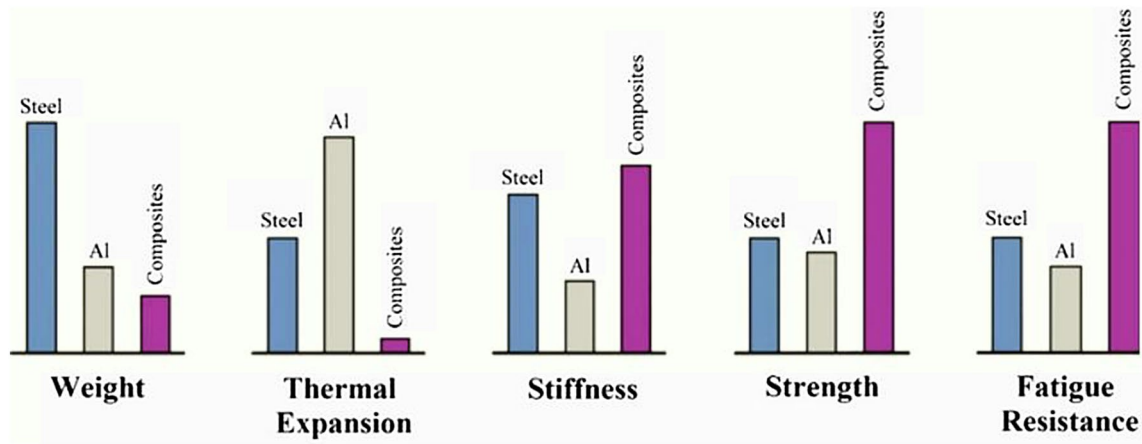


Fig. 1 Comparison of conventional and composite materials [1]

although liquid–metal infiltration, squeeze casting, rheo-casting (semisolid casting) and spray deposition have also been used [3].

Powder metallurgy is the designation specified to the process in which fine powdered materials were mixed or blended, then formed into desired shape (compacted), and then heated (sintered) in a controlled environment in order to bond or join contacting surfaces of the powders to establish the required desired properties. The process is generally known as P/M, which readily offers itself for producing small parts in masses, fabricating high-precision intricate parts, eliminating the necessity of additional finishing or machining processes [4]. There is minimal waste of material, uncommon mixtures or materials can be developed, and organized grades of permeability or porosity can be obtained. Major application areas lean toward to the places for which the P/M technique has robust commercial advantage or where desired characteristics and properties would be challenging to achieve by any further method. The process of powder metallurgy normally comprises four basic phases: powder selection, blending of powders, compacting the powders at room temperature at high pressure and sintering at elevated temperature in a controlled atmosphere. Often, when needed, some secondary processing steps are carried out optionally to acquire enhanced precision or special properties. Figure 2 shows a basic flowchart of the orthodox die-compaction P/M procedure.

With the addition of ceramic particulates as reinforcing elements in the metal matrix, the machining features change drastically, generating different kinds of chips than machining aluminum [5]. High tool wear and higher surface roughness were general while machining Al–SiC MMCs, since chips having built-up-edge chips were influenced by lower speeds and higher feeds. When MMCs were subjected to machining processes, the result will be

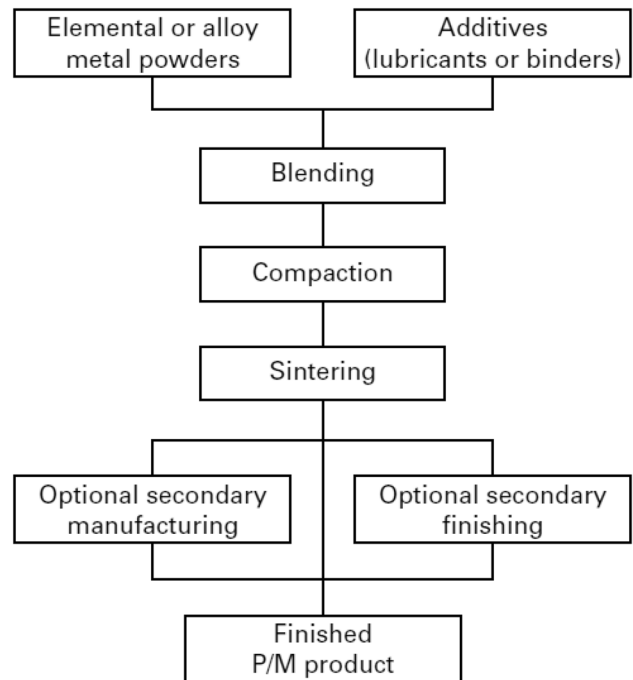


Fig. 2 Powder metallurgy process procedure

extreme tool wear and surface roughness on workpieces subjected to machining because of the occurrence of ceramic reinforcing phases in metal matrix [6]. Henceforth, cutting tools designated for machining should repel the abrasive wear action of these ceramics. Conventional high-speed steels cannot be chosen as cutting tool for machining, because of poor performance, and in due course advanced tool materials such as PCD, cemented carbide and cermets were selected. In this investigation, preliminary tests on machinability have been performed for determining the machining conditions, which favors the employing carbide cutting tools in machining ceramic

particles-reinforced MMCs [7]. In machining, principal cutting action contains shear deformation of workpiece material to form as a chip; a new layer of surface gets exposed as the material is removed as chip. For shaping materials, the frequently applied process is machining [8].

Adeosun et al. [9] reviewed different works performed on different proportions of aluminum hybrid composite and its influence on physical, mechanical and chemical properties and perceived that the degree of improvement of these composite properties intensely depends the reinforcement nature, hardness of reinforcing particles, its volume fraction, size of particle and homogeneity of dispersion of particles inside the matrix and methods of fabrication. Khaloobagheri et al. [10] fabricated copper-based composites that were reinforced with 8 mol.% yttria stabilized with different weight proportions of zirconia (8-YSZ) particles adopting powder metallurgy technique, by compacting the powders at 500 MPa and sintering at 900 °C in argon atmosphere for 2 h. Mechanical characterization of fabricated specimens shows an increase in microhardness and compressive strength with higher amount of ZrO₂ reinforcement. With an increase in zirconia content up to 5 wt% in the matrix, the composite relative densities decrease from 96.1 to 92.0%. Pal et al. [11] studied the kinetics of age-hardening P/M Al–Cu–Mg alloy reinforced with 5, 15 or 25 vol.% SiC after exposed to solution treatment. Higher hardness is sensed in 5% volume fraction SiC particles, regardless of solution treatment form, which may be due to the lowest inter-particle spacing, also due to higher volume fraction of particulates among the studied composites. Prosviryakov [12] fabricated composite material based on copper with 15–35 wt% SiC through mechanical alloying procedure in planetary mill, followed by hot pressing, and proved that an upsurge in the SiC content (till 25 wt%) and milling time lead to an improved level of hardness of the composite, because of refining of particulate reinforcing and microstructural homogenization. Increasing the content of SiC over 25 wt% (48 vol.%), with intense decline of homogeneity in microstructure and increased porosity, material hardness decreases.

Bodukuri et al. [13] prepared AMMC of Al–SiC–B₄C by sintering of mechanically ball milling procedure in powder metallurgy procedures considering three different blends of configurations in volume fractions, viz., 90%Al 8%SiC 2%B₄C, 90%Al 5%SiC 5%B₄C and 90%Al 3%SiC 7%B₄C. It is observed that the affinity to shrink through sintering process appears to get reduced with improvement in apparent density and the utmost improvement in tap density was identified during the initial tapping period and finally the tap density turns out to be constant. With decreasing percentage of boron carbide, hardness value too decreases. Pawade and Joshi [14] applied Taguchi-based grey analysis to analyze the results obtained for optimizing

Inconel 718 material during high-speed turning, considering multiple performance characteristics by combining the experimental OA with grey relational analysis. Among the tried parameters, feed rate provides the strongest relationship to surface roughness and cutting forces. The surface obtained after machining shows more modifications (microparticle deposits, smeared layer, microchip fragments and debris) at lesser cutting speed. Senthilkumar and Tamizharasan [15] performed turning operation in AISI 1045 steel to optimize the geometry of carbide inserts by applying Taguchi's technique taking into account, several performances of maximizing MRR and minimizing tool wear and roughness, and identified the noteworthy contributions using ANOVA. During machining aluminum and aluminum alloys, cutting speeds were chosen in the range of 400–1000 m/min. But for AMMC reinforced with hard ceramic particulates, lower cutting speeds produces favorable results, as previously established by most of the researchers [6, 16, 17].

Based on the literature survey conducted, it is observed that limited researchers have done machining studies on aluminum metal matrix composite reinforced with 4% copper. P/M procedure is a fast growing technology which embraces almost all alloy and metallic materials. Commonly, high-purity aluminum powders were used as matrix material to study matrix–reinforcement interface relationship more deeply, as the impurities available in the base matrix material will influence greatly interface during the production of composite. Machinability studies have been carried out by turning process, Taguchi's design of experiment (DoE) is applied for formulating the experimental trials and Taguchi's method of analysis, and signal-to-noise (S/N) ratio is applied for analyzing the chip thickness ratio (CTR).

2 Materials, methodology and experimental procedure

For fabricating the environmental-friendly composite material, the preliminary materials identified for the fabrication of MMC were 99.9 percentage pure aluminum, silicon carbide as ceramic reinforcement and addition of secondary material as copper. For weight reduction, aluminum is identified as the matrix material, which also provides the required property of ductility, and for improving the thermal conductivity of the fabricated specimens, copper is introduced into the matrix material [18], and for improving the hardness and strength of composite, silicon carbide was reinforced [19]. With improved properties of thermal conductivity and coefficient of thermal expansion, MMCs of AlSiC along with copper addition are the promising solution for electronic packaging industries and for

direct applications in rocket nozzles, brake rotors, propeller shaft, liners and calipers. The process of powder metallurgy comprises ascertaining the essential base materials, weighing up the constituents in correct quantities by volume segments and then homogenizing the materials for uniformity. The specific advantage of choosing powder metallurgy route for fabricating this composite is to attain: controlled porosity, better chemical homogeneity and uniform microstructure and of less fabrication cost. The homogenized powders were then compacted in a closed die at 20 tons, for attaining the required size and shape using a universal testing machine. After that, the sample was sintered at a temperature of 500 °C for nearly 3 h, while the furnace was upheld with an atmosphere of nitrogen of 0.5 L/min. Figure 3 shows the method of powder metallurgy procedure adopted during the composite material preparation.

For analyzing the machinability performance of the fabricated AMMC specimen of Al + 4%Cu + 7.5%SiC, a L_9 orthogonal array based on Taguchi’s technique is framed for performing the experimental trials with different arrangements of machining parameters [20]. Taguchi’s parameter design approach is used for improving the robustness of a system, assisting in product and process design decisions. Due to easy adaption and simplicity, this method can be applied for optimizing the process variables. This method provides the desired information from minimum number of trials with different number of levels. Taguchi’s methodology was applied for the three factors selected, without considering the interaction effects between them, and therefore, a L_9 orthogonal array is formulated for studying the influence of selected parameters

individually alone. If interaction effect is considered in the experiment, a higher orthogonal array must be selected. It is realized that an orthogonal array-based experiment represents the lowest possible fraction of all the possible combinations. The small size of the experiments and the fact that they seem to provide satisfactory results are the two reasons that orthogonal arrays are preferred for experimental designs. The verification of results comes from running experiments with actual parts and by carrying out confirmation tests at the predicted optimum (desirable) condition [21]. The turning features such as depth of cut, feed rate and cutting speed were analyzed to obtain optimal cutting conditions [22]. Table 1 shows the level values selected for turning process [17].

The least number of trials can be calculated as per the following equation:

$$DOF = (P - 1)(F) + (P - 1)(P - 1)(Q) + 1 \text{ for the average} \tag{1}$$

where DOF is the desired degree of freedom, F is number of independent (or) input variables, P is their chosen levels, and Q is number of interactions needed in the study. The number of experimental trials must be equal or larger

Table 1 Control factors and their values for turning

Parameter	Level		
	Level 1	Level 2	Level 3
Cutting speed (m/min)	120	150	180
Feed rate (mm/rev)	0.05	0.07	0.09
Depth of cut (mm)	0.15	0.30	0.45

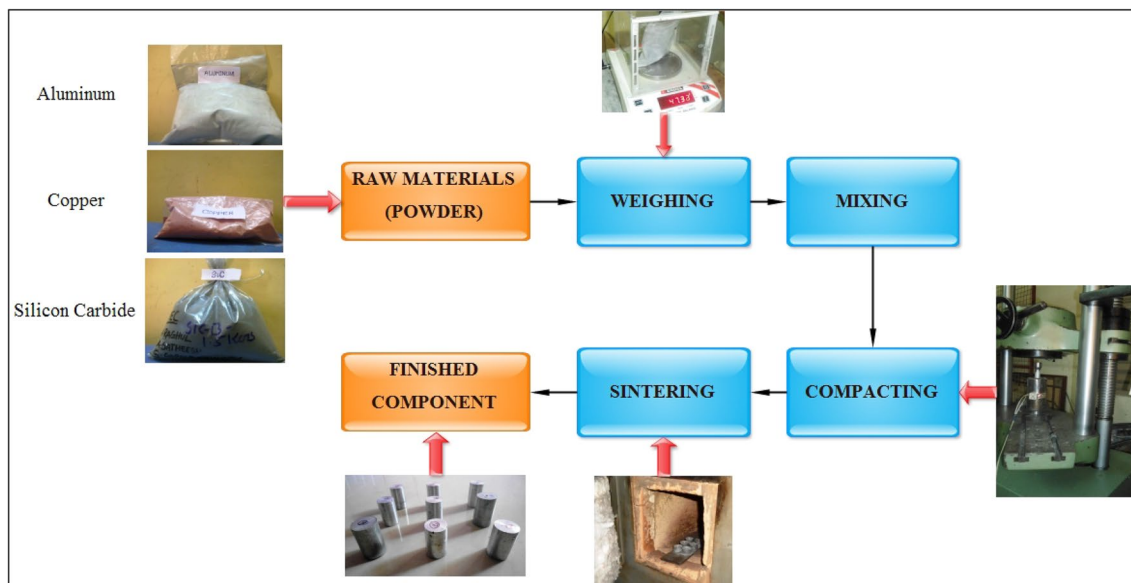


Fig. 3 AMMC production steps in P/M route

than the DOF for performing experiments in process optimization [23]. Taguchi's methodology was applied for the three factors selected without considering the interaction effect between them, and therefore, a L_9 orthogonal array is formulated for studying the influence of selected parameters individually. If interaction effect is considered in the experiment, a higher orthogonal array must be selected. Using Minitab-18, for the identified control factors and their range of level values, a L_9 orthogonal array is chosen with the help of array selector for three factors varied through three levels with no interaction effect. Orthogonal array formulated using Taguchi's DoE for different arrangements of turning is given in Table 2.

For investigation, performance characteristics are classified into three categories, namely lower-the-better, larger-the-better and nominal-the-better which is used to calculate the signal-to-noise (S/N) ratio in Taguchi's methodology [24]. The influence of external disturbances on the performance was measured through S/N ratio. For larger S/N ratio, the outputs will be highly robust against the external noise. For the category of lower-the-better, the characteristics were normally an unfavorable output and for larger-the-better condition, the characteristics were normally a favorite output, and for nominal-the-best condition, a nominal output is the quality characteristics [25].

Lower-the-better (minimize):

$$S/N = -10 \log \left(\frac{1}{n} \sum_{i=1}^n y_i^2 \right) \quad (2)$$

Larger-the-better (maximize):

$$S/N = -10 \log \left(\frac{1}{n} \sum_{i=1}^n \frac{1}{y_i^2} \right) \quad (3)$$

Nominal-the-best:

$$S/N = 10 \log \left(\frac{\bar{y}}{s_y^2} \right) \quad (4)$$

where \bar{y}_i denotes the experimentally detected value of i th experiment and n is the number of duplications of each test. The objective of smaller-the-better condition was to lower the assessment of the quality characteristics to the possible smaller value to zero, a target or ideal value, e.g., surface roughness, cutting forces and tool wear, etc. The concept of larger-the-better was applied when a situation arises to improve the quality characteristics values as much as possible such as productivity, tool life and MRR. Nominal-the-best is useful when an ultimate or target value is indicated toward the quality characteristics such as clearances and dimensional tolerances [26].

The nomenclature of uncoated carbide cutting insert selected for turning the AMMC specimens was TNMG 120404. The trials were performed on the CNC Turning center, Lokesh model 2 axis CNC TL-20 with a swing diameter of 350 mm, distance among the centers was 600 mm with spindle speed of 4500 rpm, and power of motor is 11 kW, which is shown in Fig. 4.

3 Results and discussion

Figure 5 shows the P/M specimens fabricated for studying the machinability behavior by turning process. The micrograph of Al-4%Cu-7.5%SiC sample displays roughly unfused/undissolved free copper in aluminum matrix with 0.6% by volume. The remaining matrix demonstrates some fine-fused Cu-Al₂ in solid solutions of aluminum [27]. Uniform distribution of SiC particulates is witnessed and was seen as dark gray particles.

Table 2 Formulated L_9 inner array for turning AMMC

Trial no.	Input values		
	Cutting speed (m/min)	Feed rate (mm/rev)	Depth of cut (mm)
1	120	0.05	0.15
2	120	0.07	0.30
3	120	0.09	0.45
4	150	0.05	0.30
5	150	0.07	0.45
6	150	0.09	0.15
7	180	0.05	0.45
8	180	0.07	0.15
9	180	0.09	0.30



Fig. 4 Lokesh TL-20 CNC turning centre

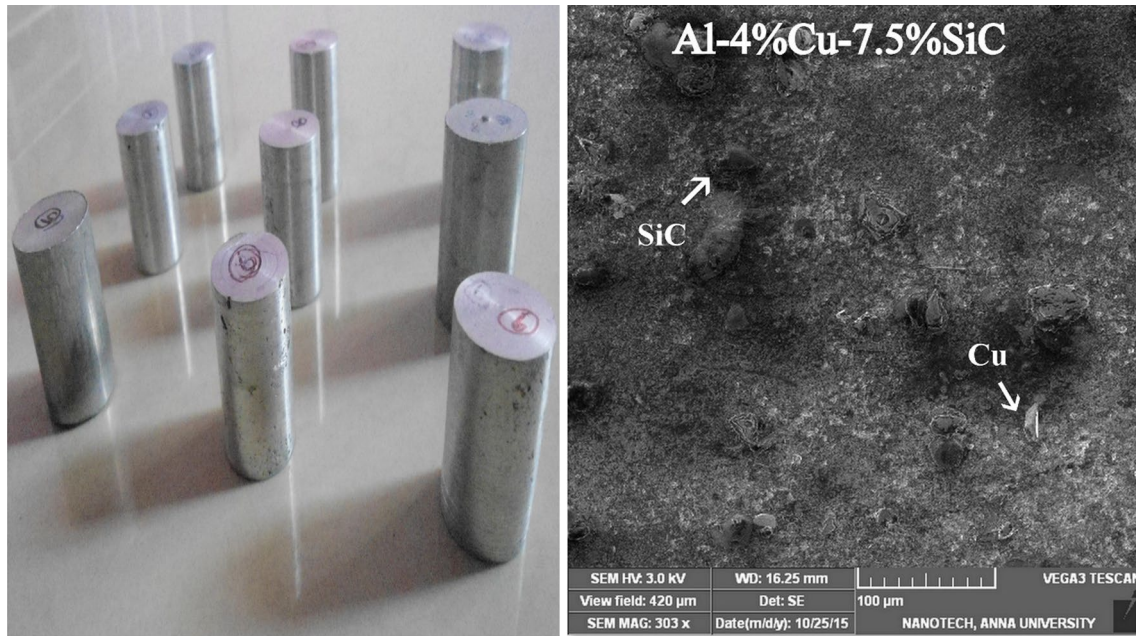


Fig. 5 SEM micrographs of Al-4%Cu-7.5% SiC MMC

Practically, all the factors (tool nose radius, feed rate, cutting speed and depth of cut) considered in turning process have indirect and direct impacts on the thickness of the metal remove (chips) during shearing. Chip thickness is a factor used to realize the elementary process of metal cutting. A lesser chip thickness suggests an improved lubrication at the tool–chip contact surface and development of chips of thinner segment, i.e., if the chip thickness declines, the process efficiency gets improved [28].

Around World War II, the official study of chip formation was encouraged. The form and nature of chips developed is an important index of machining because it directly or indirectly specifies: workpiece nature and behavior, specific energy requirement and level of interaction at the chip–tool interfaces. The CTR is geometrically related to the tool rake angle and the shear plane angle [29]. For higher CTR, the shear plane angle is smaller, where the chip moves away slowly, whereas a large shear plane angle means a thin CTR, producing high-velocity chips. CTR reduces rapidly with increase in speed, with rapid reduction in chip stiffness. The shape of the chip depends primarily on the work material, cutting regime, and tool material and geometry. Hence, chip study is inevitable in turning process [30]. Both low friction and high rake angles lead to low chip thickness ratios. High work hardening rates are also found experimentally to lead to higher chip thickness ratios [31]. Smaller value of coefficient of friction indicates that the shear angle is larger which results in smaller shear plane area that provides benefits of lower cutting force needed to shear off the chips and

lower cutting temperature being generated during the machining process. Discontinuous chips were characterized by high tool-chip friction, and continuous chips were produced by low tool-chip friction. By reducing the friction angle or coefficient of friction, the shear plane angle is increased, and therefore, CTR is reduced [32].

Experiments were performed under dry machining condition, without the use of coolant, in order to eliminate the harmful effects of coolant, thereby reducing the impacts on environment. Chips were obtained after completing each trial, and chip thickness was measured from slider caliper. Table 3 shows the uncut chip thickness, thickness of chip and calculated chip thickness ratio for all experimental conditions. It was identified that an increase

Table 3 Chip thickness ratio for machining conditions

Exp. no.	Uncut chip thickness (t)	Chip thickness (t_c)	Chip thickness ratio ($r_t = t/t_c$)	S/N ratio (LTB)
1	0.36	0.82	0.44	7.131
2	0.39	0.79	0.49	6.196
3	0.45	0.85	0.53	5.514
4	0.37	0.78	0.47	6.558
5	0.42	0.8	0.52	5.680
6	0.33	0.76	0.43	7.331
7	0.30	0.72	0.42	7.535
8	0.26	0.75	0.35	9.119
9	0.29	0.77	0.38	8.404

in cutting speed increases the chip thickness, but gets increased with increasing depth of cut and feed rate [33].

Experiments were shepherded in a CNC machining centre, with the formulated OA. Throughout the turning trials, a single workpiece and carbide insert were used for individual experimental condition and the resultant outputs were measured. The experiments were conducted twice (two replications) for the purpose of minimizing the experimental errors, and for analysis, mean values were considered.

The surface plot and perturbation plot for CTR for the selected independent factors are shown in Fig. 6. Observation shows that CTR increases with increase in cutting speed in an exponential manner, whereas feed rate has a curvilinear effect; CTR increases with increase in feed

rate. A linear trend of an increase in CTR is observed with increase in depth of cut. Perturbation plot is used for comparing the influences of factors in the common design space, where CTR is plotted by varying one parameter over the selected range, maintaining other factors constant. A steep slope obtained for cutting speed and depth of cut shows that CTR is more sensitive toward these factors, whereas a relatively flat line of feed rate shows that CTR is insensitive toward feed rate.

For analyzing the CTR, lower-the-better concept of Taguchi's S/N ratio was applied as given in Eq. (2). The calculated S/N ratio is given in Table 3. Interpretations from the experimental outcome show as the cutting speed is increased, decrease in CTR was found, and with increasing depth of cut, CTR further increases. But with variation in

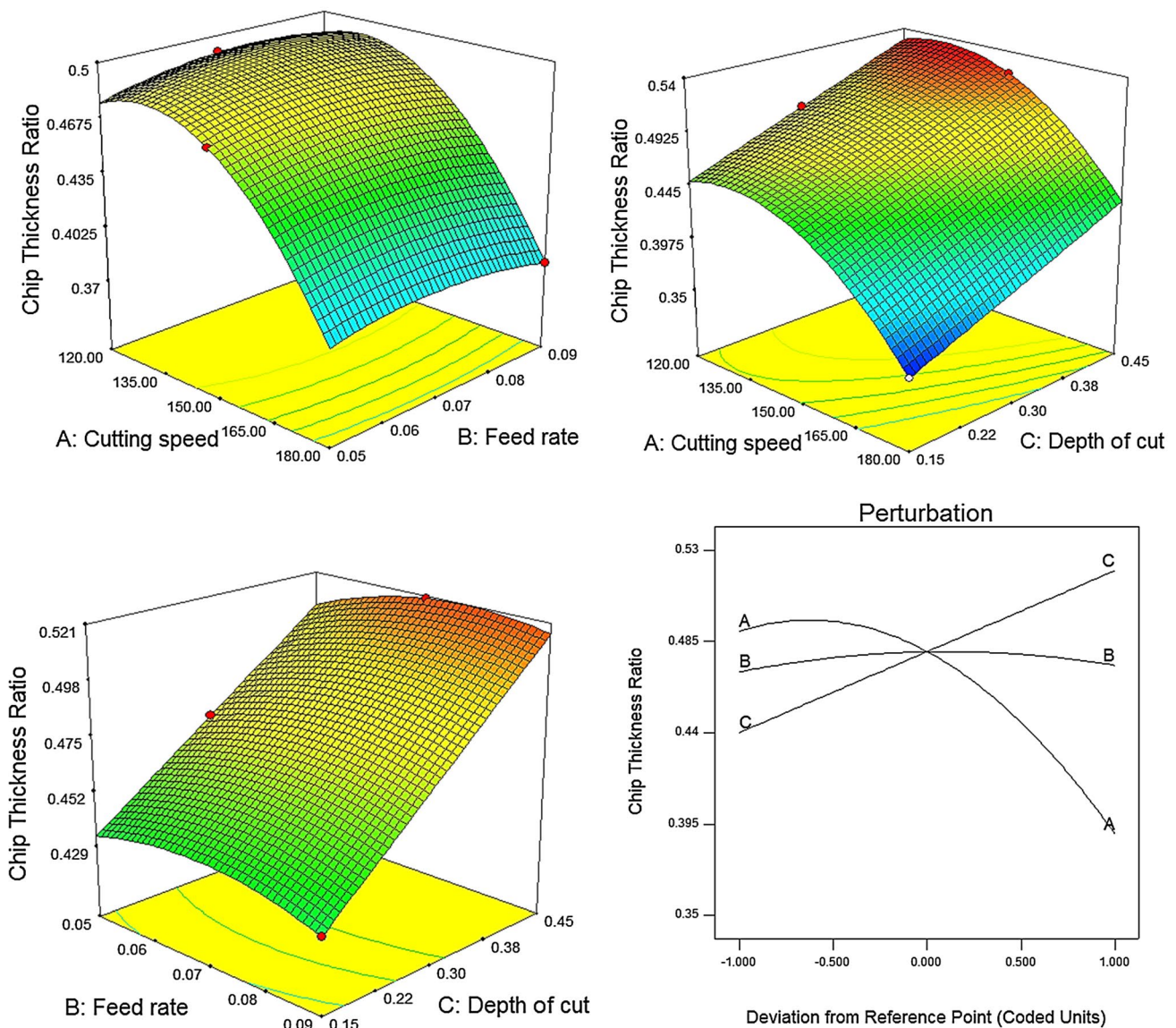


Fig. 6 Surface plot and perturbation plot of CTR

feed rate from 0.05 to 0.07 mm/rev, chip thickness ratio rises and after that, it decreases with increase in feed rate to 0.09 mm/rev. Macro-images of obtained chip are shown in Fig. 7, captured for high speed, medium speed and low speed conditions through optical microscope. Rough structure is observed with fused edges when the speed is high along with higher depth of cut and also for medium speed and medium depth of cut, whereas a perfect continuous chip is produced with lower speed and lower depth of cut [34].

The machined surfaces of the Al + 4%Cu + 7.5%SiC P/M specimens for different machining conditions are studied using optical microscopes in the as-polished and as-etched conditions. Figure 8 shows the turned surface for experiment condition 1 in which the as-polished matrix shows the free copper which has dissolved in the metal matrix during sintering process. The eutectic copper Cu–Al₂ is observed in the polished matrix as dark particles. The etched matrix shows the precipitation of Cu–Al₂ eutectic particles at the grain boundaries of primary aluminum

grains. The grain size of the primary is measured 200 μm. The presence of eutectic at the grain boundaries showed dissolution of copper and formation of Cu–Al₂.

The surface of the turned P/M specimen is shown in Fig. 9; as-polished matrix condition shows the presence of copper dissolved and the formed eutectics of Cu–Al₂ by the metal matrix during sintering process. On the other hand, more dissolved and formed Cu–Al₂ eutectic particles are observed in the matrix of aluminum. Some distributed SiC grains were available in matrix. The lower percentage addition of SiC showed large and fine free SiC particles. The grain size is between 25 and 35 μm. No pores between the grains are observed, and the fusion of the metal matrix has taken place. The etched matrix shows the precipitation of Cu–Al₂ eutectic particles at the grain boundaries of primary aluminum grains. The grain size of the primary is measured about 175 μm. The presence of eutectic at the grain boundaries showed dissolution of copper and formation of Cu–Al₂. The uniformly distributed composite particles of SiC are present at the grain boundary and

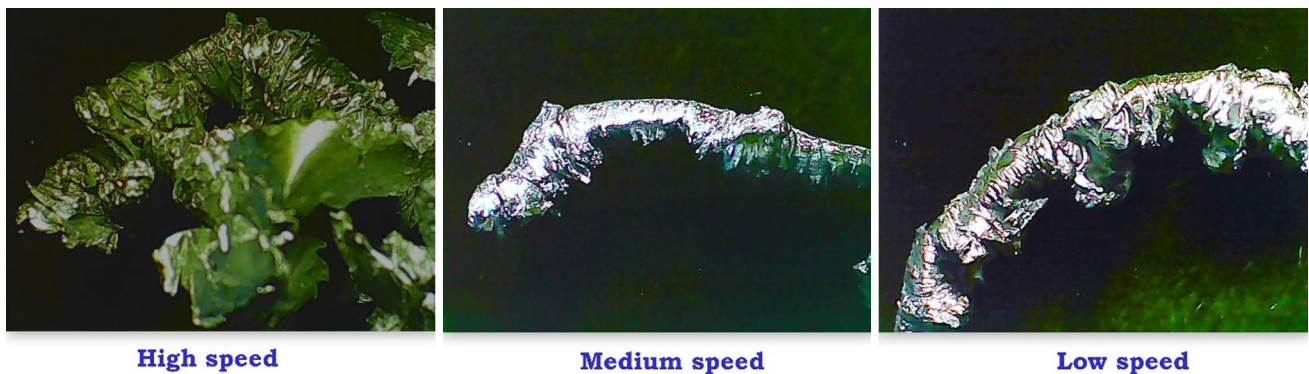


Fig. 7 Macro-graphs of formed chips

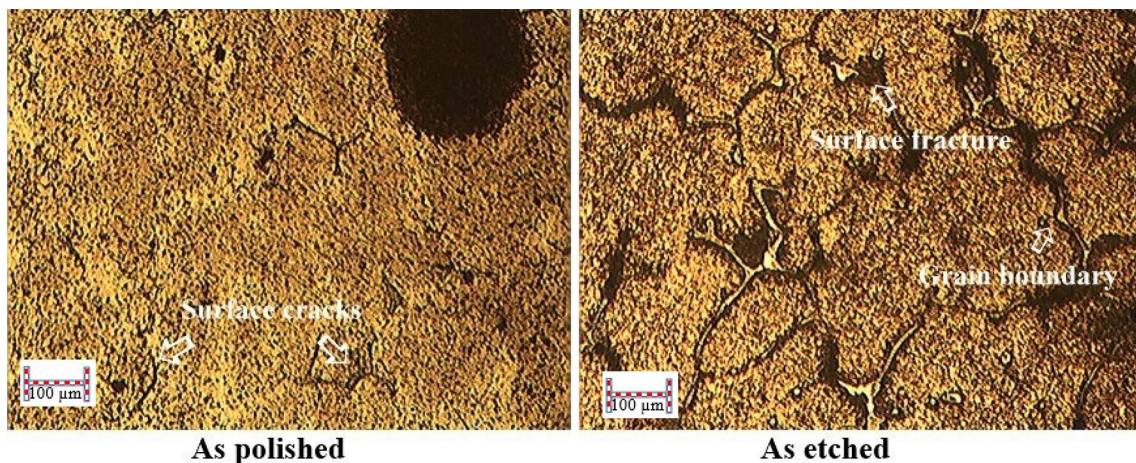


Fig. 8 Turned surface for Exp. No. 1

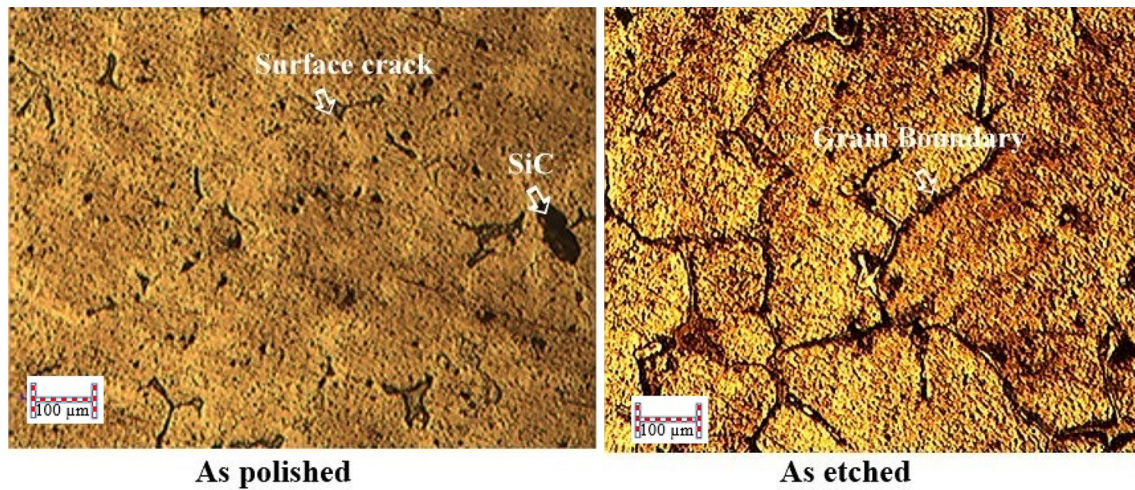


Fig. 9 Turned surface for Exp. No. 3

inside the grain boundaries. No voids are observed around the grains of SiC in the metal matrix.

In Fig. 10, the as-polished photo-micrograph shows the completely dissolved metal matrix with no pores in the sintered matrix. The SiC particulates were not observed in aluminum matrix. The etched matrix shows the photo-micrograph of metal matrix composite with the precipitation of grain boundary eutectic Cu–Al₂ in primary aluminum grains. The grain size is ranging between 175 and 200 μm.

For experiment condition 7, the turned surface is shown in Fig. 11; the polished matrix shows the distribution of composite particulates of silicon carbide was homogeneous in the metal matrix of aluminum. The dissolution of copper is complete, and no free copper is observed. The etched matrix showed the

photo-micrograph of metal matrix composite by powder metallurgical process (compacting and sintering). The fusion of the matrix is seen, and the composite particles were dispersed in matrix. The eutectic Cu–Al₂ is present at the grain boundaries of primary aluminum grains. The composite particulates were available inside the grains and at the grain boundary of primary aluminum grains. The grain size is measured as 150 μm.

The chips obtained during the turning process are collected for analysis from the nine experiments, and some of the chips are shown in Fig. 12, and the CTR was calculated for all the conditions. From chip examination observations, lower cutting speed, depth of cut and feed rate produce continuous curled chips and with increase in cutting speed, discontinuous chips were produced.

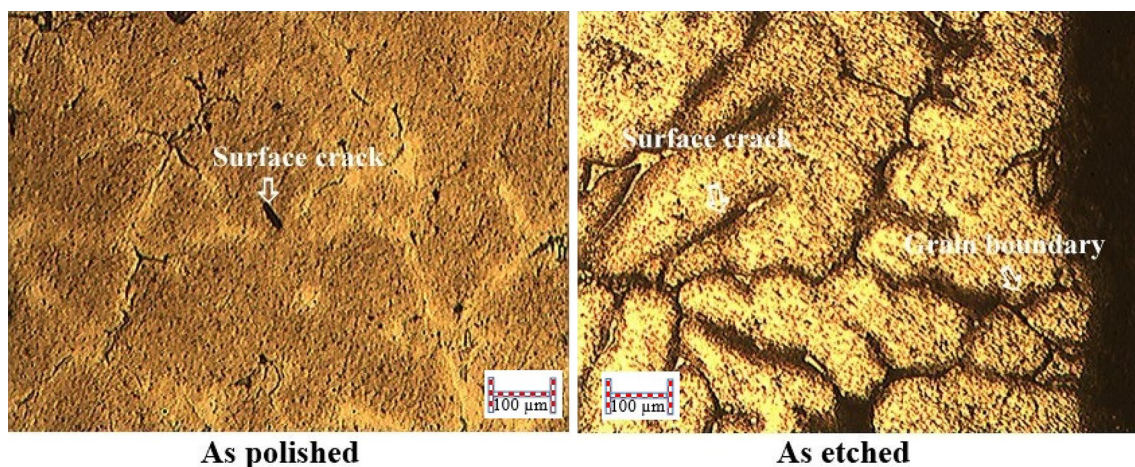


Fig. 10 Turned surface for Exp. No. 5

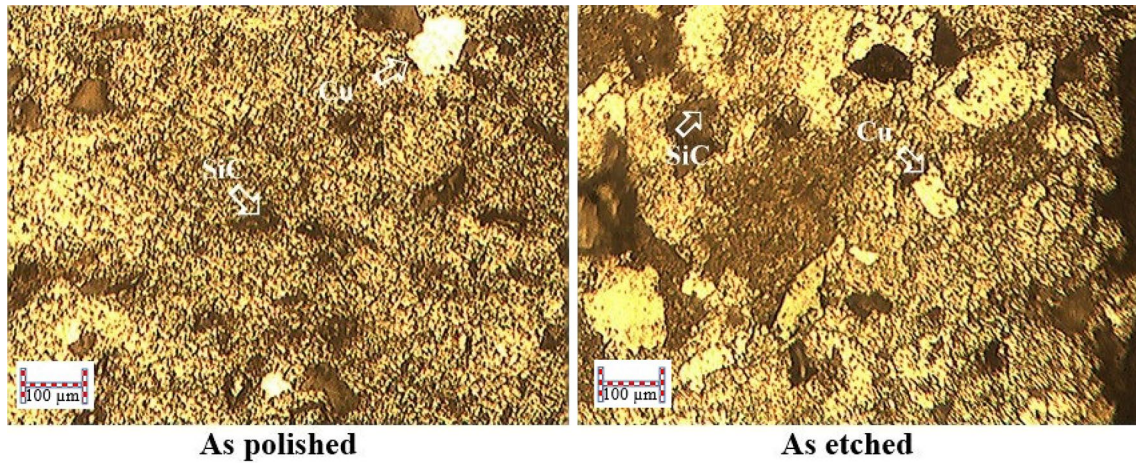


Fig. 11 Turned surface for Exp. No. 7

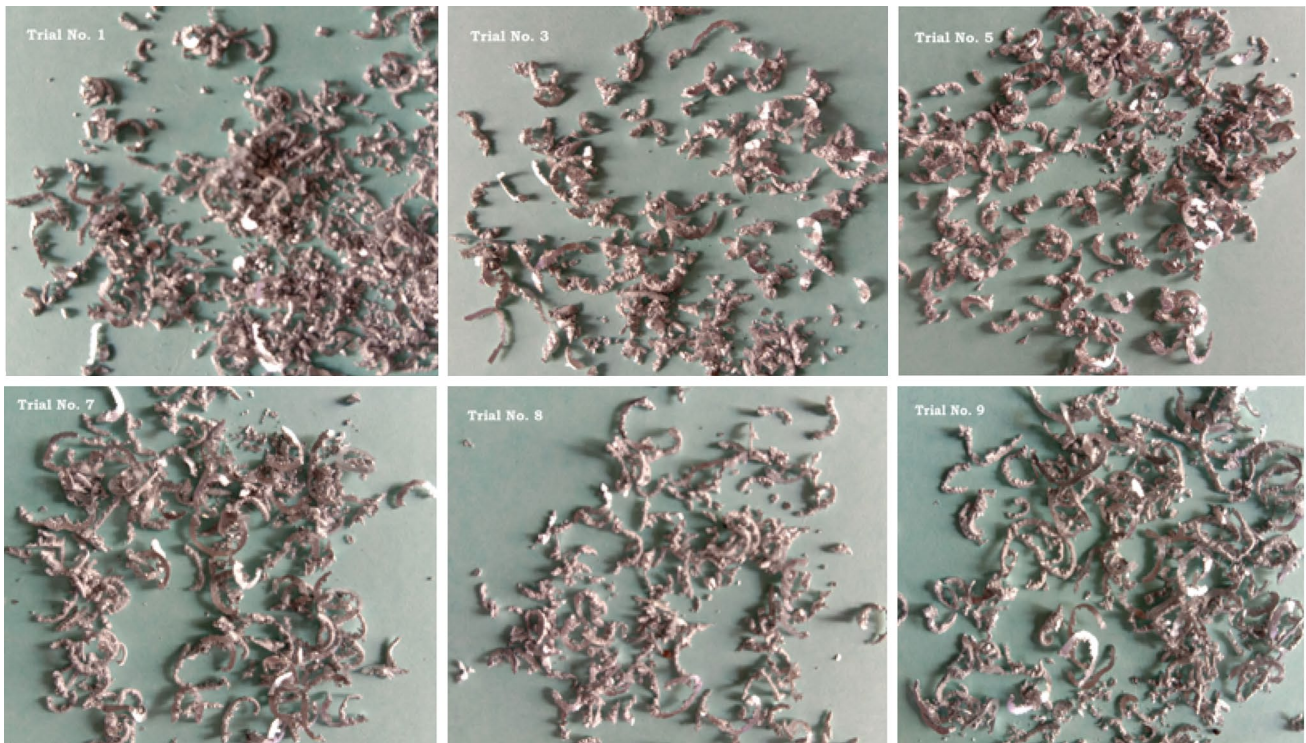


Fig. 12 Chips obtained during turning process

The size of the chip depends on the feed and depth given during machining [35].

Response table for CTR, given in Table 4, was calculated by averaging the S/N ratio values given in Table 3 for each and every level value of the chosen input parameters [36]. Observation shows that influence of cutting speed is higher, followed by depth of cut and feed rate based on the rank given for the highest deviation as from Table 4.

Table 4 Response table for chip thickness ratio

Factors	Level 1	Level 2	Level 3	Max – min	Rank
Cutting speed	6.281	6.523	8.353	2.072	1
Feed rate	7.075	6.998	7.083	0.085	3
Depth of cut	7.860	7.053	6.243	1.617	2

The response plot for CTR was drawn based on the response table, as presented in Fig. 13. From response plot and table, the optimum condition for lower CTR was identified as follows: cutting speed value of 180 m/min, feed rate value of 0.09 mm/rev and depth of cut value of 0.15 mm.

With the usage of linear graphs, the influence of selected input variables on the measured responses will be effortlessly studied. When the correlation between two input factors considered over output responses is denoted by parallel strokes, it is established that no collaboration exists between the selected input factors [37]. If their association is characterized by non-parallel lines, it is clinched that a noticeable association occurs among that two dependable input factors. Figure 14 shows the influence of various inputs over the CTR. It was witnessed that a significant interaction effect occurs amid feed rate and cutting speed and also among depth of cut and feed rate. But in between cutting speed and depth of cut, no interaction effect was perceived, as seen by straight parallel lines. Hence, when feed rate combines with the other two input parameters, it influences the CTR ratio to a larger extent.

From analysis of variance, a statistical way of analyzing experimental data, investigators have acknowledged the variables that were allotted as independent and dependent variables. Independent and dependent factors were closely connected to each other. Dependent variables were alleged to be prejudiced or influenced by the selected independent variables. Subject to the category of examination, it is important to identify which factors have noteworthy consequence on the response and quantify the variability in response variable that is attributable toward each variable [38]. ANOVA performed on the CTR demonstrates that cutting speed

was the supreme favorable parameter which contributes over the response by 64.13%, trailed by depth of cut over 35.26% and feed rate that much makes any impact on the chip thickness ratio, as shown in Table 5. The R^2 is 99.92% and R^2 (adj.) is 99.70%, and R^2 (Pred.) of 98.48% shows that the developed model is a good one. Since ANOVA is performed on 95% confidence interval, the obtained R^2 value is much better for analysis.

3.1 Validation experiment with optimum settings

With the obtained optimum condition of cutting speed level value of 180 m/min, feed rate level value of 0.09 mm/rev and depth of cut level value of 0.15 mm, a verification trial was executed in the similar investigational arrangement and the CTR was calculated as 0.347, which is lower by 22.51% toward the average value of experimental results. The S/N ratio of the confirmation experiment CTR is 9.193. For authenticating the confirmed result, the assessed mean of Taguchi S/N ratio is calculated as $A_3B_2C_1$.

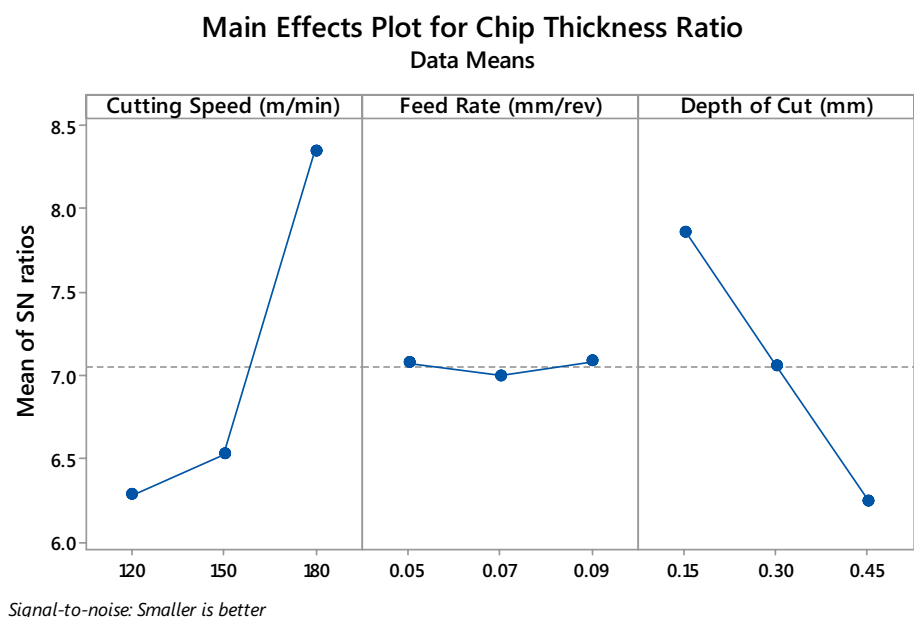
$$SNR_{em} = V_{3m} + F_{3m} + D_{1m} - 2SNR_m \tag{4}$$

where SNR_{em} = estimated mean of signal-to-noise ratio; V_{3m} = mean S/N ratio conforming to cutting speed, V_3 ; F_{3m} = mean S/N ratio conforming to feed rate, F_3 ; D_{1m} = mean S/N ratio conforming to depth of cut, D_1 ; SNR_m = overall mean of signal-to-noise ratio; SNR_{con} = signal-to-noise ratio of confirmation experiment.

From Table 4, the average values for the chosen input factors were determined and are substituted in Eq. (4).

$$SNR_{em} = 8.353 + 7.083 + 7.860 - (2 * 7.052) = 9.192.$$

Fig. 13 Response plot for chip thickness ratio



Interaction Plot for Chip thickness ratio Data Means

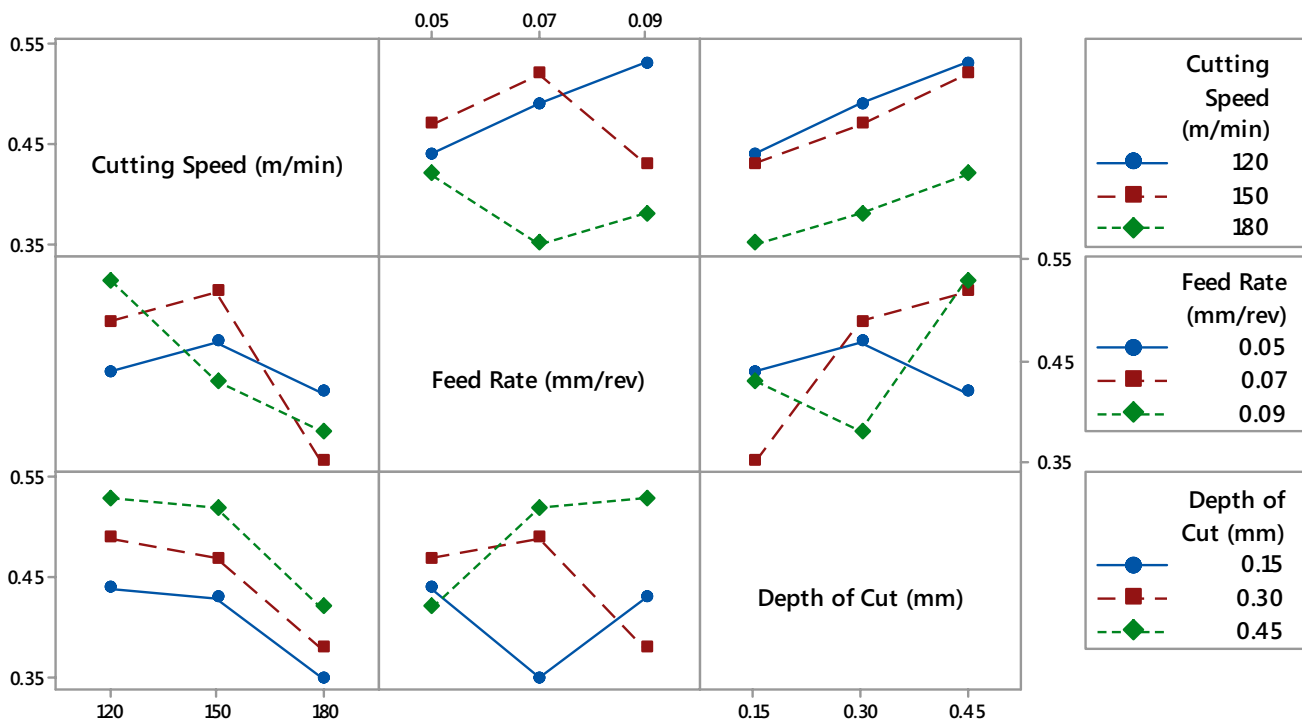


Fig. 14 Linear graphs for chip thickness ratio

Table 5 ANOVA for chip thickness ratio

Source	DF	Adj. SS	Adj. MS	F value	P value	% Contribution
Cutting speed	2	0.018956	0.009478	853.00	0.001	64.13
Feed rate	2	0.000156	0.000078	7.00	0.125	0.53
Depth of cut	2	0.010422	0.005211	469.00	0.002	35.26
Error	2	0.000022	0.000011			0.07
Total	8	0.029556				

3.2 Determination of confidence interval

For predicting the S/N ratio of confirmation experiment, confidence interval (CI) is applied [39], which is determined from Eq. (5).

$$CI = \sqrt{F_{0.05}(3, f_e) V_e \left[\frac{1}{n} + \frac{1}{R} \right]} \tag{5}$$

where f_e —error degrees of freedom (2) from Table 5, $F_{0.05}(3, f_e)$ —F ratio required for risk (3, 2) = 19.16 from standard “F” table, V_e —error variance (0.000011) from Table 5, R —number of repetitions for confirmation test (1), N —total number of experiments ($n_r \times$ number of experiments) = $1 \times 9 = 9$ [n_r —number of replications (1)], n —effective number of

replications = $N / (1 + \text{degrees of freedom associated with chip thickness ratio from Table 5}) = 9 / (1 + 8) = 1$.

From the aforementioned relations, the assessment of CI for S/N ratio is determined as:

$$CI = \{ 19.16 \times 0.000011 [(1/1) + (1/1)] \}^{1/2} = 0.021.$$

The 95% CI of the optimal factor settings S/N ratio obtained from the validation experiment is as follows:

$$(SNR_{em} - CI) < SNR_{con} < (SNR_{em} + CI) \tag{6}$$

The outcome of confirmation test indicates that the S/N ratio lies in within the range $(SNR_{em} - CI)$ and $(SNR_{em} + CI)$. (i.e., 9.193 lies within the range of 9.171 and

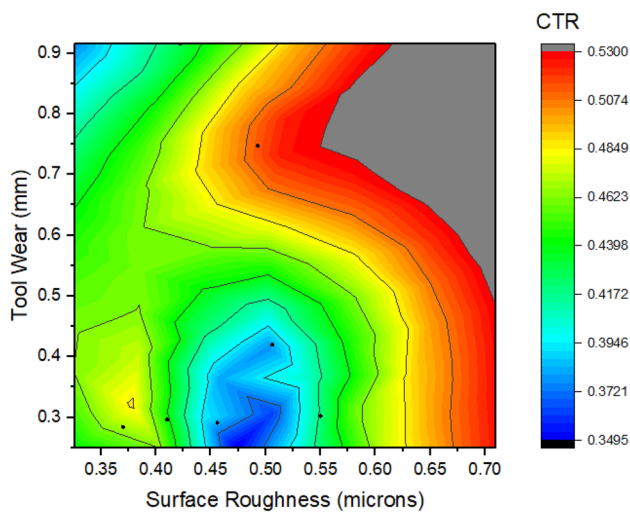


Fig. 15 Relationship contour among output responses

9.213). The confirmed Taguchi S/N ratio is consequently established by these calculations.

3.3 Correlation between CTR, tool wear and surface roughness

A contour plot also called as level plot is a graphical procedure of representing a three-dimensional surface by plotting constant z slices (iso-response values), known as contours, in a two-dimensional format. This plot graphs two predictor variables on the x - and y -axes and a response variable Z as contours. Figure 15 shows the contour plot for three dependent variables CTR, tool wear and surface roughness. Inferences made from the contour plot identify three major regions for different conditions. Lower CTR is acquired with lower tool wear, and subsequently, lower surface roughness is achieved where the friction between tool–workpiece interface is lower. Higher CTR is characterized with higher tool wear and surface roughness. Hence, it is obvious that CTR increases with increase in tool wear and surface roughness. Tool wear is characterized by higher friction and higher temperatures at the interfaces, which damages the machining surface through drastic shear deformation in the form of chips with saw-tooth structure, thereby increasing the CTR.

4 Conclusion

Machining test in CNC turning centre with uncoated carbide cutting inserts on turning Al–4%Cu–7.5%SiC was examined. Macro-examination and micro-examination were employed for studying the chip morphology, and

the CTR was evaluated for analysis. Conclusions obtained from the analysis were as follows:

- It was found that chip thickness gets reduced with rise in cutting speed, but rises with increase in depth of cut and feed rate. Macro-images of the chip show rough structure with fused edges when the speed is high and medium, whereas a perfect continuous chip is produced with lower speed.
- Micro-analysis performed with optical microscope shows surface cracks on machined surface with clear visible grain boundaries for all conditions. With higher feed and speed, higher cracks were seen.
- Using Taguchi's approach, the optimum condition for lower CTR obtained was cutting speed value of 180 m/min, 0.09 mm/rev feed rate with 0.15 mm depth of cut. Interaction plot shows a significant interaction effect exists among cutting speed and feed rate and also among feed rate and depth of cut.
- From ANOVA with an R^2 value of 99.92%, cutting speed was identified as the most influential factor which contributes by 64.13%, trailed by depth of cut by 35.26%, while the influence of feed rate was negligible.
- For validating the obtained optimum parameter settings, a verification experiment was carried out and the obtained chip thickness ratio was verified by calculating the confidence interval. The calculated S/N ratio of 9.193 lies in between 9.171 and 9.213 of determined confidence interval levels, which makes the results trustworthy.
- From contour plot, three major regions were identified for the obtained CTR. Lower CTR is acquired with lower tool wear, and subsequently, lower surface roughness and higher CTR were characterized with higher tool wear and surface roughness due to high friction at the interfaces. It is identified that CTR increases with increase in tool wear and surface roughness.

Compliance with ethical standards

Conflict of interest The authors declare that they have no conflict of interest.

References

1. Deutsch S (1978) Automotive applications for advanced composite materials. In: Proceedings of the 23rd national SAMPE symposium, p 34
2. Arslan G, Kalemantas A (2009) Processing of silicon carbide–boron carbide–aluminium composites. *J Eur Ceram Soc* 29(3):473–480
3. Davis JR (1999) Corrosion of aluminum and aluminum alloys. ASM International, Materials Park

4. Klar E (1998) Powder metal technologies and applications, vol 7. ASM International, Materials Park
5. Singh S, Kumar S, Kumar S (2016) Analysis of chip thickness ratio while machining of EN-8D steel. *Int J Eng Technol Manag Appl Sci* 3:55–60
6. Astakhov VP (2011) Machining of hard materials—definitions and industrial applications. In: Davim JP (ed) *Machining of hard materials*. Springer, New York, pp 1–32
7. Kalpakjian S, Schmid SR (2001) *Manufacturing engineering and technology*. Prentice-Hall, New York
8. Groover MP (2010) *Fundamentals of modern manufacturing—materials, processes and systems*. Wiley, New York
9. Adeosun SO, Osoba LO, Taiwo OO (2014) Characteristics of aluminum hybrid composites. *Int J Chem Mol Nucl Mater Metall Eng* 8(7):737–744
10. Khaloobagheri M, Janipour B, Askari N, Abad ESK (2013) Characterisation of powder metallurgy Cu–ZrO₂ composites. *Adv Prod Eng Manag* 8(4):242–248
11. Pal S, Mitra R, Bhanuprasad VV (2008) Aging behaviour of Al–Cu–Mg alloy–SiC composites. *Mater Sci Eng A* 480:496–505
12. Prosviryakov AS (2015) SiC content effect on the properties of Cu–SiC composites produced by mechanical alloying. *J Alloys Compd* 632:707–710
13. Bodukuri AK, Eswaraiyah K, Rajendar K, Sampath V (2016) Fabrication of Al–SiC–B₄C metal matrix composite by powder metallurgy technique and evaluating mechanical properties. *Perspect Sci* 8:428–431
14. Pawade RS, Joshi SS (2011) Multi-objective optimization of surface roughness and cutting forces in high-speed turning of Inconel 718 using Taguchi grey relational analysis (TGRA). *Int J Adv Manuf Technol* 56:47–62
15. Senthilkumar N, Tamizharasan T (2014) Experimental investigation of cutting zone temperature and flank wear correlation in turning AISI 1045 steel with different tool geometries. *Indian J Eng Mater Sci* 21(2):139–148
16. Hashmi MSJ (2017) *Comprehensive materials finishing, volume 1: Finish machining and net-shape forming*. Elsevier, Toronto
17. Walsh RA (2001) *Handbook of machining and metalworking calculations*. McGraw-Hill, New York
18. Rajaram G, Kumaran S, Rao TS (2011) Influence of graphite and copper in mechanical properties of aluminum silicon alloy. *Trans Indian Inst Met* 64(1–2):53–56
19. Rahman MH, Rashed HMMA (2014) Characterization of silicon carbide reinforced aluminum matrix composites. *Proc Eng* 90:103–109
20. Selvakumar V, Muruganandam S, Tamizharasan T, Senthilkumar N (2016) Machinability evaluation of Al–4%Cu–7.5%SiC metal matrix composite by Taguchi–Grey relational analysis and NSGA-II. *Sadhana* 41(10):1219–1234
21. Roy RK (2001) *Design of experiments using the Taguchi approach: 16 steps to product and process improvement*. Wiley, New York
22. Senthilkumar N, Ganapathy T, Tamizharasan T (2014) Optimization of machining and geometrical parameters in turning process using Taguchi method. *Aust J Mech Eng* 12(2):233–246
23. Muthuramalingam T, Mohan B (2014) Application of Taguchi-grey multi responses optimization on process parameters in electro erosion. *Measurement* 58:495–502
24. Senthilkumar N, Tamizharasan T, Anandakrishnan V (2014) An hybrid Taguchi-grey relational technique and cuckoo search algorithm for multi-criteria optimization in hard turning of AISI D3 steel. *J Adv Eng Res* 1(1):16–31
25. Ross PJ (2005) *Taguchi techniques for quality engineering*. Tata McGraw Hill, New Delhi
26. Senthilkumar N, Selvakumar V, Tamizharasan T (2016) Optimization and performance analysis of uncoated and coated carbide inserts during hard turning AISI D2 steel using hybrid GRA–PCA technique. *Appl Mech Mater* 852:151–159
27. Selvakumar V, Muruganandam S, Senthilkumar N (2016) Evaluation of mechanical and tribological behavior of Al–4%Cu–x%SiC composites prepared through powder metallurgy technique. *Trans Indian Inst Met* 70(5):1305–1315
28. Thamizhmanii S, Hasan S (2012) Machinability study using chip thickness ratio on difficult to cut metals by CBN cutting tool. *Key Eng Mater* 504–506:1317–1322
29. Trent EM (2016) *Metal cutting*. Butterworths, London
30. Astakhov VP (2006) *Tribology of metal cutting*. Elsevier, Oxford
31. Childs THC, Maekawa K, Obikawa T, Yamane Y (2000) *Metal machining theory and applications*. Elsevier, Oxford
32. Natasha AR, Othman H, Ghani JA, Hassan C, Haron C, Syarif J (2014) Chip formation and coefficient of friction in turning S45C medium carbon steel. *Int J Mech Mechatron Eng* 14(6):89–92
33. Davim JP (2012) *Machining of metal matrix composites*. Springer, London
34. Sreenivasulu R (2016) Taguchi based optimization for surface roughness and chip thickness during end milling process on aluminium 6351-T6 alloy. *Indep J Manag Prod* 7(4):1212–1226
35. Santos MC Jr, Machado AR, Barrozo MAS, Jackson MJ, Ezugwu EO (2015) Multi-objective optimization of cutting conditions when turning aluminum alloys (1350-O and 7075-T6 grades) using genetic algorithm. *Int J Adv Manuf Technol* 76(5–8):1123–1138
36. Jaiganesh V, Yokesh Kumar B, Sevel P, Balaji AJ (2018) Optimization of process parameters on commercial mild steel using Taguchi technique. *Int J Eng Technol* 7(1.1):138–142
37. Tamizharasan T, Senthilkumar N (2012) Analysis of surface roughness and material removal rate in turning using Taguchi's technique. In: *Proceedings of the international conference on advances in engineering, science and management*, pp 231–236
38. Gamst G, Meyers LS, Guarino AJ (2008) *Analysis of variance designs—a conceptual and computational approach with SPSS and SAS*. Cambridge University Press, Cambridge
39. Senthilkumar N, Tamizharasan T, Anandakrishnan V (2014) Experimental investigation and performance analysis of cemented carbide inserts of different geometries using Taguchi based grey relational analysis. *Measurement* 58:520–536